Supplementary Material for

A continuum state variable theory to model the size-dependent surface energy of nanostructures

S1. Continuum-based framework

We denote ∇, Div and ∇^2 as the gradient, divergence and Laplacian operators, respectively. The magnitude of a vector $\mathbf{b}$ is denoted by $|\mathbf{b}|$. The scalar product between two vectors $\mathbf{a}$ and $\mathbf{b}$ is denoted by $\mathbf{a}\cdot\mathbf{b}$. In our continuum theory, $\mathcal{R}$ represents the region occupied by a continuum body in three-dimensional space with vector $\mathbf{n}$ being the outward unit normal on its boundary denoted by $\mathcal{S}$. The area element and volume element of the body is denoted by dA and dV, respectively. For the sake of transparency, we develop our theory under *isothermal* conditions and in the absence of deformation, body forces, and heat fluxes/sources.

S1.1. Micro-force balance

For the surface effect variable λ, the micro-force system which describes the forces that perform work associated to changes in the atomic arrangement caused by the creation of a free surface consist of: (a) the micro-traction vector, $\mathbf{c}$, measured per unit area, and (b) the scalar *internal* micro-force, π^{int}, measured per unit volume. As a first-cut approach, we assume that the *external* micro-force vanishes [1].

Following the methodology of Gurtin [1], we write the micro-force balance equation as

$$\int_{\mathcal{S}} \mathbf{c}\cdot\mathbf{n}\,\mathrm{dA} = \int_{\mathcal{R}} \pi^{int}\,\mathrm{dV}. \tag{S1}$$

Applying the divergence theorem in Eq. S1 and localizing the result within $\mathcal{R}$ results in

$$\mathrm{Div}\,\mathbf{c} = \pi^{int}. \tag{S2}$$

S1.2. Balance of energy

With the vector $\mathbf{m} = \nabla\lambda$, recall that the Helmholtz free energy per unit volume, $\psi = \hat{\psi}(\lambda, \mathbf{m})$. The first law of thermodynamics is given by

$$\int_{\mathcal{S}} (\mathbf{c}\cdot\mathbf{n})\,\dot{\lambda}\,\mathrm{dA} = \overset{\cdot}{\int_{\mathcal{R}} \epsilon\,\mathrm{dV}} \tag{S3}$$

where ϵ represents the internal energy per unit volume. With η and $\theta > 0$ representing the entropy per unit volume and the absolute temperature, respectively, we have

$$\epsilon = \psi + \eta\theta \quad\Longrightarrow\quad \dot{\epsilon} = \dot{\psi} + \dot{\eta}\theta \tag{S4}$$

under isothermal conditions i.e. $\dot{\theta} = 0$. Along with the use of Eqs. S2 and S4$_2$, we apply the divergence theorem in Eq. S3 and localize the result within $\mathcal{R}$ to obtain

$$\mathbf{c}\cdot\dot{\mathbf{m}} + \pi^{int}\dot{\lambda} - \dot{\eta}\theta = \dot{\psi} = \frac{\partial\psi}{\partial\lambda}\dot{\lambda} + \frac{\partial\psi}{\partial\mathbf{m}}\cdot\dot{\mathbf{m}}. \tag{S5}$$

S1.3. Dissipation inequality

We write the second law of thermodynamics as

$$\overset{\cdot}{\int_{\mathcal{R}} \eta\,\mathrm{dV}} \geq 0. \tag{S6}$$

Localizing inequality S6 within $\mathcal{R}$, and then multiplying both sides of the localized inequality by θ yields

$$\dot{\eta}\theta \geq 0. \tag{S7}$$

Substituting Eq. S5 into inequality S7 results in the *dissipation inequality*

$$\left(\mathbf{c} - \frac{\partial\psi}{\partial\mathbf{m}}\right)\cdot\dot{\mathbf{m}} + \left(\pi^{int} - \frac{\partial\psi}{\partial\lambda}\right)\dot{\lambda} \geq 0. \tag{S8}$$

S1.4. Reduced dissipation inequality

Substituting $\psi = (1/2)\omega\lambda^2 + (1/2)\kappa\left|\mathbf{m}\right|^2$ into inequality S8 and using standard continuum thermodynamics arguments yield $\mathbf{c} = \dfrac{\partial\psi}{\partial\mathbf{m}} = \kappa\mathbf{m}$, and the *reduced dissipation inequality*

$$\Gamma = \left(\pi^{int} - \omega\lambda\right)\dot{\lambda} \geq 0 \tag{S9}$$

where Γ represents the non-negative *dissipation density*. To rule out trivial cases, we assume that the atomic rearrangement process caused by the creation of a free surface is *strictly* dissipative [2]. Hence, inequality S9 then reduces to

$$\left(\pi^{int} - \omega\lambda\right)\dot{\lambda} > 0 \quad \text{for } \dot{\lambda} \neq 0. \tag{S10}$$

S1.5. Driving force for atomic rearrangement & kinetic relation

Let $f^{\lambda} \equiv \pi^{int} - \omega\lambda$ represent the *driving force* for atomic rearrangement caused by the creation of a free surface. To satisfy inequality S10, we take $f^{\lambda} = \beta\dot{\lambda}$ where $\beta > 0$ denotes the damping coefficient (with units of force per unit velocity) for the atomic rearrangement process caused by the creation of a free surface. Using Eqs. S2 and $\mathbf{c} = \kappa\mathbf{m}$ then results in the kinetic relation

$$\dot{\lambda} = \beta^{-1} f^{\lambda} = \beta^{-1}\left\{\pi^{int} - \omega\lambda\right\} = \beta^{-1}\left\{\mathrm{Div}\,\mathbf{c} - \omega\lambda\right\} = \beta^{-1}\left\{\kappa\nabla^2\lambda - \omega\lambda\right\}. \tag{S11}$$

Once *steady-state* conditions are achieved, the surface effect variable will cease to evolve i.e. $\dot{\lambda} = 0$. Hence, the characteristic equation at steady-state is then given by

$$\dot{\lambda} = \beta^{-1}\left\{\kappa\nabla^2\lambda - \omega\lambda\right\} = 0 \implies l_s^2\,\nabla^2\lambda - \lambda = 0 \tag{S12}$$

where $l_s = \sqrt{\kappa/\omega}$ represents the *characteristic length scale* for the atomic rearrangement process caused by the presence of the free surface. Generally, l_s can depend on type of material, structure (crystalline/amorphous) and crystal orientation.

S2. Equilibration process of the surface effect variable field

S2.1. One-dimensional simulations

Consider a three-dimensional solid plate of thickness h_f. Let axis$-z$ denote the thickness direction of the plate. We impose periodic boundary conditions on this plate in all directions for time $t < 0$. This plate is also taken to occupy the space spanning coordinates $z = -h_f/2$ to $z = +h_f/2$ along axis$-z$. Since periodic boundary conditions are imposed on the plate in all directions, we set $\lambda = 0$ throughout the plate for time $t < 0$. The periodic boundary conditions imposed on the plate in direction-z are released for time $t \geq 0$, and therefore the plate has a free surface at planes $z = \pm h_f/2$ for time $t \geq 0$.

We shall numerically simulate the equilibration process of the surface effect variable field within the plate for time $t \geq 0$. Let the normalized coordinate along the $z-$axis, $\bar{z} = z/l_s$, the characteristic time, $\tau = \beta/\omega$, and the normalized time, $\bar{t} = t/\tau$. For the present case, Eq. S11 can be reduced to the one-dimensional non-dimensionalized form

$$\frac{\mathrm{d}\lambda}{\mathrm{d}\bar{t}} = \frac{\mathrm{d}^2\lambda}{\mathrm{d}\bar{z}^2} - \lambda. \tag{S13}$$

The equilibration process of the surface effect variable field can be modeled by a phase field-like simulation via the discretization of Eq. S13 in time and space. We have implemented the time and space discretization of Eq. S13 into MATLAB [3] to perform the phase field-like simulations. For our numerical simulations, we impose: (a) the boundary conditions $\lambda = 1$ at $\bar{z} = \pm\dfrac{h_f}{2l_s}$, and (b) the initial conditions $\lambda = 0$ at $\bar{t} = 0$ for $-\dfrac{h_f}{2l_s} < \bar{z} < +\dfrac{h_f}{2l_s}$. The numerical simulations are stopped once the surface effect variable field has equilibrated i.e. the surface effect variable field has reached a steady-state profile.

Fig. S1 shows the equilibration process of the surface effect variable field for $h_f = 16l_s$ i.e. for a relatively thin plate. Using Eq. 11 of the main part of the paper, we have also plotted the steady-state solution for the surface effect variable field for $h_f = 16l_s$ in Fig. S1. The numerical simulation results show that the surface effect variable field has equilibrated at approximately $\bar{t} = 4.0$. From the numerical simulation results plotted in Fig. S1, we can see that the equilibration process of the surface effect variable starts from the free surface and then progresses towards the center of the plate.

We have also performed a numerical simulation for a relatively thick plate i.e. $h_f = 100l_s$, and Fig. S2 shows the equilibration process of the surface effect variable field for $h_f = 100l_s$. As previously done, we also use Eq. 11 of the main part of the paper and plot the steady-state solution for the surface effect variable for $h_f = 100l_s$ in Fig. S2. The numerical simulation results show that the surface effect variable field has equilibrated at approximately $\bar{t} = 3.5$. From the results shown in Fig. S2, we can see that for a relatively thick plate, major atomic rearrangement is confined to the regions in the very near vicinity of the free surface, and the interior region of the relatively thick plate undergoes very minimal or effectively negligible atomic rearrangement due to the presence of the free surface.

S2.2. Two-dimensional simulations

Consider a three-dimensional solid plate which has in-plane dimensions of $h_f \times h_f$, measured along axes$-x$ and y. We impose periodic boundary conditions on this plate in all directions for time $t < 0$. This plate is also taken to occupy the space spanning coordinates $x = -h_f/2$ to $x = +h_f/2$ along axis$-x$, and $y = -h_f/2$ to $y = +h_f/2$ along axis$-y$. Since periodic boundary conditions are imposed on the plate in all directions, we set $\lambda = 0$ throughout the plate for time $t < 0$. The periodic boundary conditions imposed on the plate in directions-x and y are released for time $t \geq 0$, and therefore the plate has a free surface at planes $x = \pm h_f/2$ and $y = \pm h_f/2$ for time $t \geq 0$.

We shall numerically simulate the equilibration process of the surface effect variable field within the plate for time $t \geq 0$. Let the normalized coordinate along the $x-$axis, $\bar{x} = x/l_s$, the normalized coordinate along the $y-$axis, $\bar{y} = y/l_s$, the characteristic time, $\tau = \beta/\omega$, and the normalized time, $\bar{t} = t/\tau$. For the present case, Eq. S11 can be reduced to the two-dimensional non-dimensionalized form

$$\frac{\mathrm{d}\lambda}{\mathrm{d}\bar{t}} = \frac{\mathrm{d}^2\lambda}{\mathrm{d}\bar{x}^2} + \frac{\mathrm{d}^2\lambda}{\mathrm{d}\bar{y}^2} - \lambda. \tag{S14}$$

The equilibration process of the surface effect variable field can be modeled by a two-dimensional phase field-like simulation via the discretization of Eq. S14 in time and space. We have implemented the time and space discretization of Eq. S13 into MATLAB [3] to perform the two-dimensional phase field-like simulations. For our numerical simulations, we impose: (a) the boundary conditions $\lambda = 1$ at $\bar{x} = \pm\dfrac{h_f}{2l_s}$ and $\bar{y} = \pm\dfrac{h_f}{2l_s}$, and (b) the initial conditions $\lambda = 0$ at $\bar{t} = 0$ for $-\dfrac{h_f}{2l_s} < \bar{x} < +\dfrac{h_f}{2l_s}$ and $-\dfrac{h_f}{2l_s} < \bar{y} < +\dfrac{h_f}{2l_s}$. The numerical simulations are stopped once the surface effect variable field has equilibrated i.e. the surface effect variable field has reached a steady-state profile.

Fig. S3 shows the equilibrated profile of the surface effect variable in plates of dimensions $100l_s \times 100l_s$ (plate A) and $25l_s \times 25l_s$ (plate B), measured along axes-x and y. For plate A, we can see that major atomic rearrangement is confined to the regions in the very near vicinity of the free surface but the interior region of plate A undergoes very minimal or effectively negligible atomic rearrangement due to the presence of the free surface. However, for plate B, it can be clearly seen that major atomic rearrangement occurs in the region in the near vicinity of the free surface and also a relatively large region in the interior portion of plate B due to the presence of the free surface. Furthermore, from the contour plots shown in Fig. S3, we can also determine from visual inspection that the average value of the surface effect variable within plate B is larger than the average value of the surface effect variable within plate A. These results are not surprising since plate B has a smaller size compared to plate A, and therefore we can conclude that the average value of the surface effect variable within a structure is *positively* correlated to the surface-to-volume ratio of the structure.

S3. Comparison between continuum theory and other theoretical models

Bhatt et al. [4] utilized a thermodynamic model and parameters obtained from DFT simulations to investigate the size dependent surface energy of selectively-oriented single crystal anatase TiO_2 nanoparticle. Fig. S4 shows the analytical model of Bhatt et al. [4] for the size dependent surface energy of (110), (103), (100)-oriented single crystal anatase TiO_2 nanoparticle as a function of nanoparticle diameter. Using $\gamma_s^\infty = \gamma_s^\infty(110) = 1.09\text{Jm}^{-2}$, $\gamma_s^\infty = \gamma_s^\infty(103) = 0.83\text{Jm}^{-2}$ and $\gamma_s^\infty = \gamma_s^\infty(100) = 0.54\text{Jm}^{-2}$, we can see from Fig. S4 that for a given single crystal orientation, our continuum theory i.e. Eq. 17 is able to accurately fit the analytical model of Bhatt et al. [4]. It is also important to note that we have used $l_s = 1.747\text{nm}$ in all of our results in Fig. S4.

References

[1] M. Gurtin, Physica D **92**, 178 (1996).
[2] L. Anand, M. Gurtin, Int. J. Solids Struct. **40**, 1465 (2003).
[3] MATLAB and Statistics Toolbox 2014, The MathWorks, Inc., Natick, Massachusetts, US.
[4] P. Bhatt, S. Mishra, P. Jha, A. Pratap, Physica B **461**, 101 (2015).

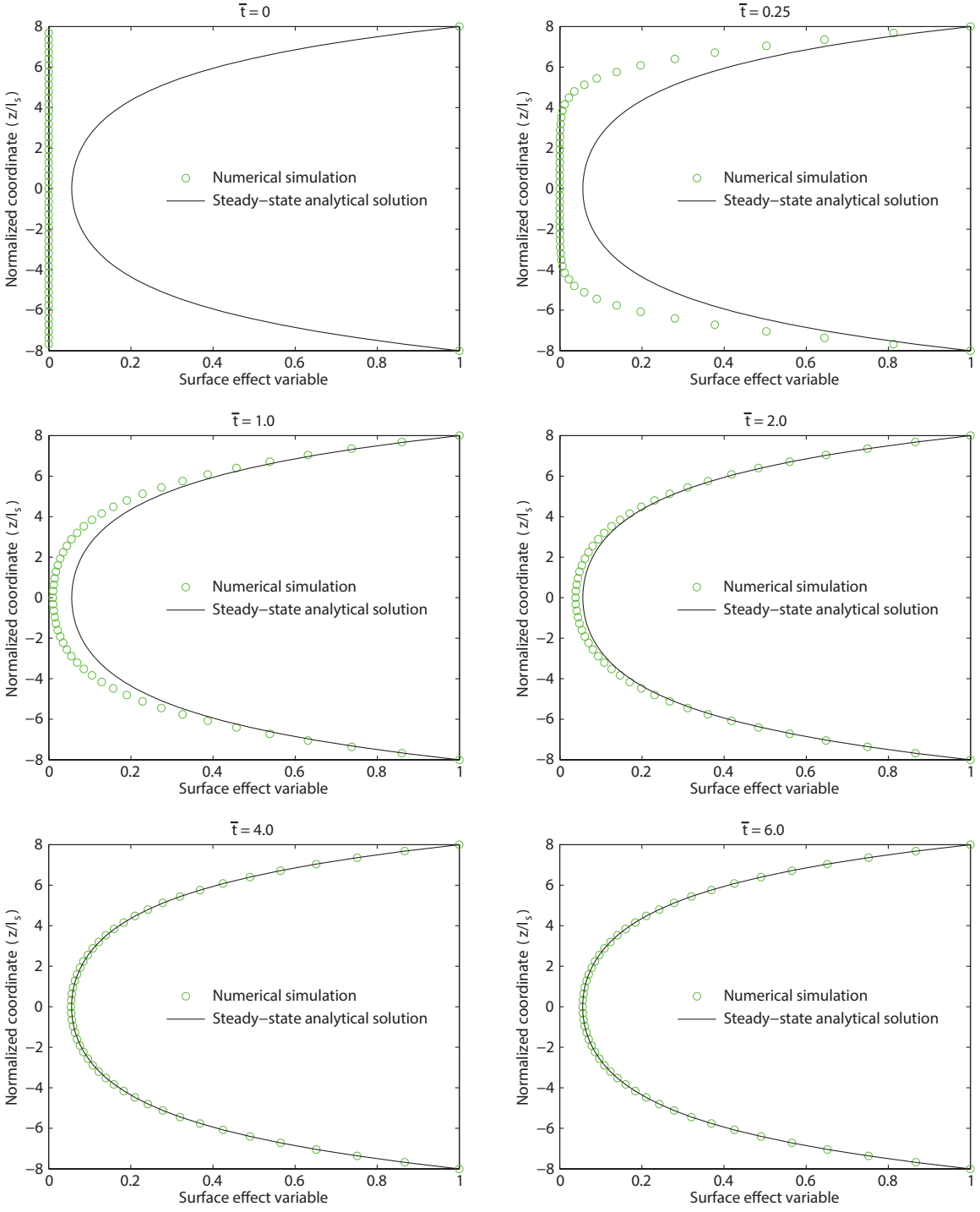

Figure S1: The numerical simulation of the equilibration process of the surface effect variable field for $h_f = 16l_s$. The numerical simulation was conducted using $l_s = \sqrt{5}$ arbitrary units and $\tau = 10$ arbitrary units.

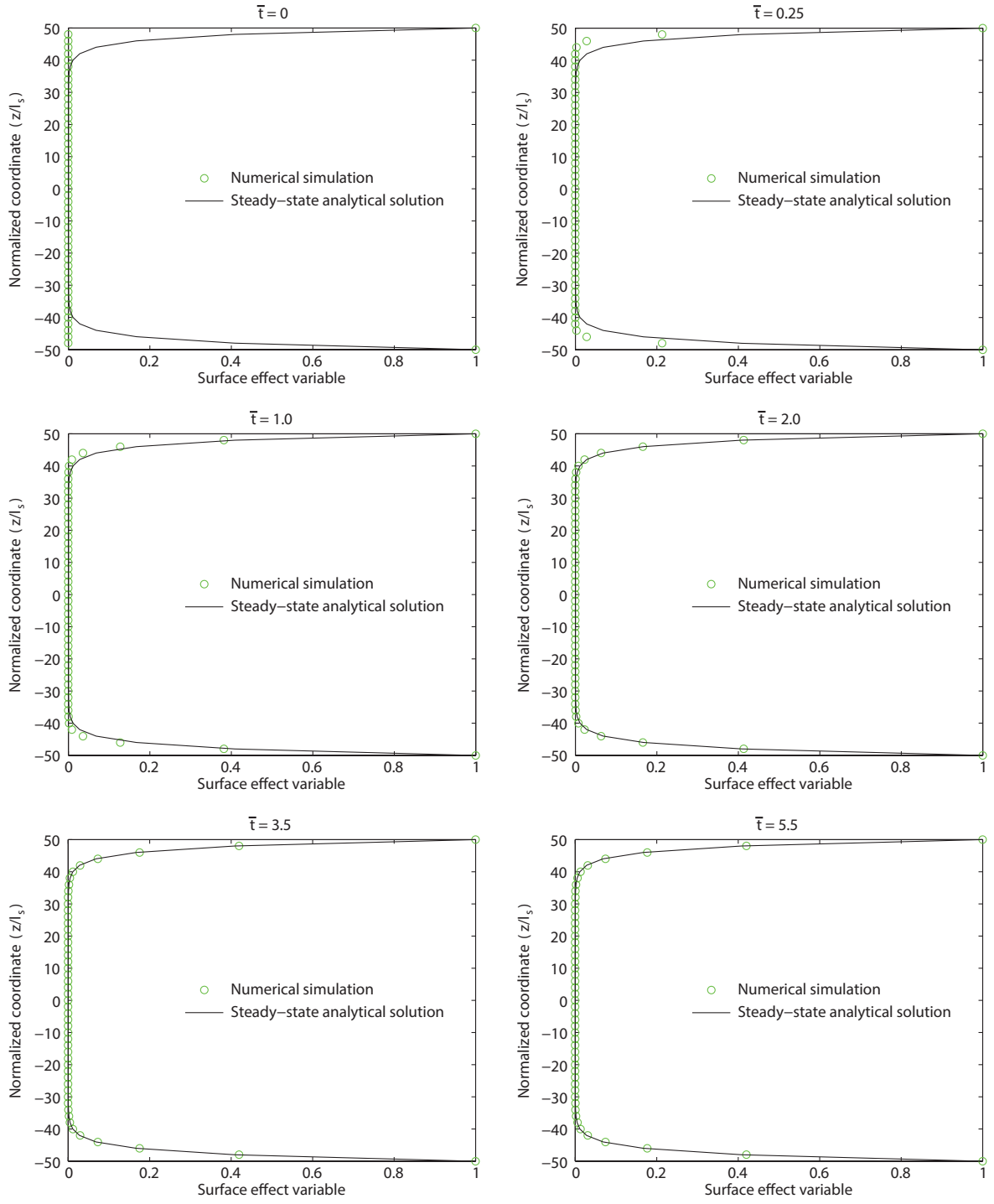

Figure S2: The numerical simulation of the equilibration process of the surface effect variable field for $h_f = 100l_s$. The numerical simulation was conducted using $l_s = \sqrt{5}$ arbitrary units and $\tau = 10$ arbitrary units.

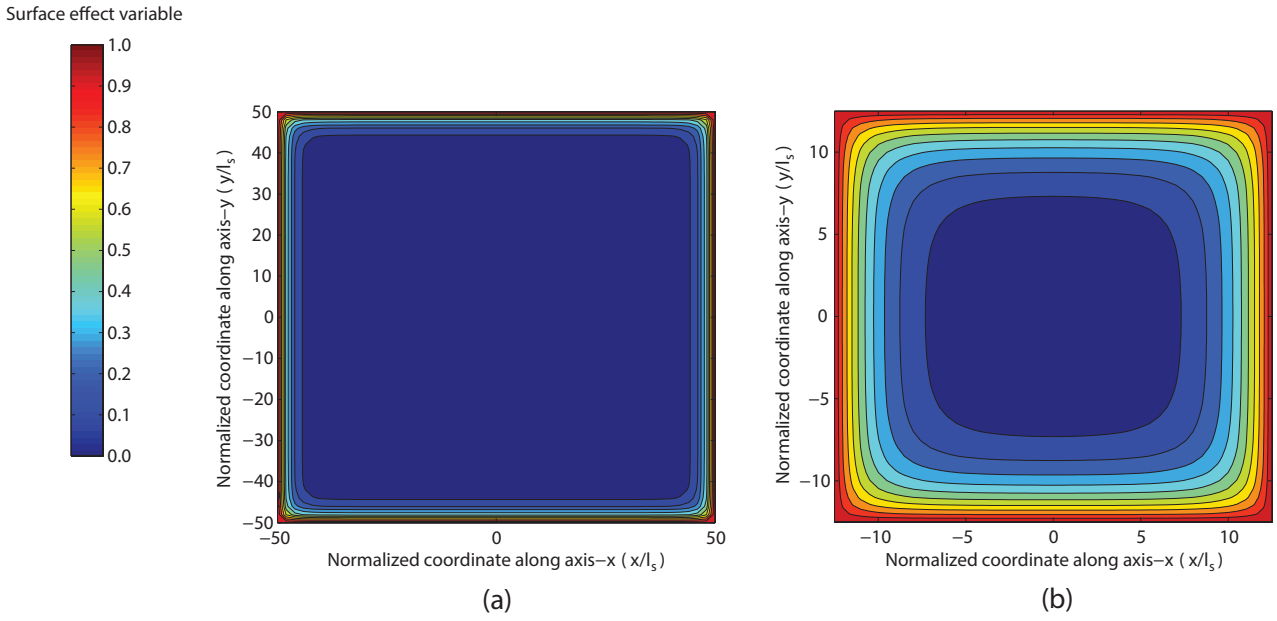

Figure S3: The equilibrated profile of the surface effect variable field in a plate of dimensions (a) $100l_s \times 100l_s$ and (b) $25l_s \times 25l_s$, measured along axes-x and y. The numerical simulations were conducted using $l_s = \sqrt{5}$ arbitrary units and $\tau = 10$ arbitrary units.

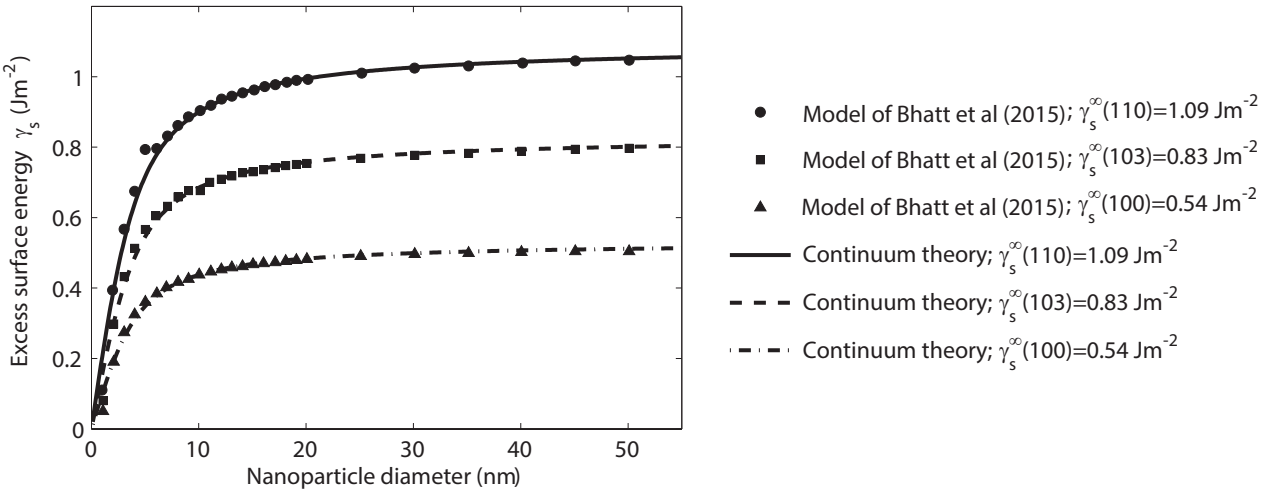

Figure S4: Size dependent surface free energy of (110), (103), (100)-oriented single crystal anatase TiO_2 nanoparticle as a function of nanoparticle diameter with $\gamma_s^\infty = \gamma_s^\infty(110) = 1.09\text{Jm}^{-2}$, $\gamma_s^\infty = \gamma_s^\infty(103) = 0.83\text{Jm}^{-2}$ and $\gamma_s^\infty = \gamma_s^\infty(100) = 0.54\text{Jm}^{-2}$. A value of $l_s = 1.747$nm is chosen in our continuum theory i.e. Eq. 17 to fit the analytical model of Bhatt et al. [4] for each single crystal orientation.